BUTTERWORTH HEINEMANN

Polymer Vol. 36 No. 1, pp. 149–154, 1995

0032-3861/95/$10.00+0.00

Complex miscibility behaviour for polymer blends in flow

M. L. Fernandez and J. S. Higgins*
Chemical Engineering Department, Imperial College of Science, Technology and Medicine, London SW7 2BY, UK

and R. Horst and B. A. Wolf
Institut für Physikalische Chemie, Johannes-Gutenberg-Universität, Jakob-Welder-Weg 13, D55099 Mainz, Germany
(Received 3 May 1994; revised 4 August 1994)

Experimental observations of the effect of shear flow on the miscibility of binary polymer blends are compared to calculations based on a generalized Gibbs energy of mixing $G_{\dot{\gamma}}$. This mixing free energy characterizes the steady state established at shear rate $\dot{\gamma}$, as the sum of G_Z, the equilibrium Gibbs energy and E_S, the energy the system stores while flowing.

(Keywords: shear; polymer blends; miscibility)

INTRODUCTION

There exists now an impressive literature on the understanding of polymer blend miscibility[1,2] and the kinetics of spinodal decomposition[3–8] in binary polymer blends under quiescent conditions. Recently there has been growing interest in the effect of flow fields on polymer mixtures and solutions. In polymer solutions[9–11] both shear-induced mixing and shear-induced demixing have been observed, unlike small molecule mixtures where only the former is reported. The literature on flow effects in polymer–polymer mixtures is still relatively sparse[12–25]. Of particular interest is the fact that relatively large shifts in miscibility limits have been reported for shear rates as low as $1\,s^{-1}$. Both flow-induced mixing and demixing have been observed but the former phenomenon greatly outweighs the latter in its frequency of occurrence. Reviews of the relevant literature are found in references 9, 10 and 24.

The phase separation behaviour of flowing systems can be easily described by introducing[26] a generalized Gibbs free energy of mixing $G_{\dot{\gamma}}$ which accounts for the energetic consequences of flow[26]. Compared to mixtures of low-molecular-mass components, polymeric systems store large amounts of energy until they reach the steady state. This stored energy E_S is considered as a perturbation of the Gibbs energy of mixing of the stagnant system G_Z, so $G_{\dot{\gamma}}$ can be evaluated according to:

$$G_{\dot{\gamma}} = G_Z + E_S \tag{1}$$

Consequently the chemical potential μ is also changed: A term has to be added that also incorporates[27] the derivative of E_S with respect to the mole fraction x_B. The coexistence conditions, based on the fact that the chemical potential of each substance (indicated by subscripts A and B) has to be the same in every phase (indicated by ′ and ″), become:

$$\mu'_A + [E'_S - (\partial E_S/\partial x_B)' x'_B] = \mu''_A + [E''_S - (\partial E_S/\partial x_B)'' x''_B] \tag{2}$$

$$\mu'_B + [E'_S + (\partial E_S/\partial x_B)'(1 - x'_B)] = \mu''_B + [E''_S + (\partial E_S/\partial x_B)''(1 - x''_B)] \tag{3}$$

This approach has been successful in describing the experimental results of polymer solutions[11]. In addition, the results of measurements on polymer blends have recently been reproduced theoretically[27,28]. As we will show in this paper, all the effects of flow which have been observed can be explained. These include shear-induced mixing, shear-induced demixing and eulytic points[11]; two inversions of the effects with varying shear rate[27] and predictions of closed miscibility gaps[28].

In several previous references[19,23,25] we have reported the effect of miscibility limits when a partially miscible polymer blend is heated into the two-phase region while it is being subjected to simple shear flow. The onset of the two-phase behaviour was observed in a light scattering apparatus and these measurements were complemented by others on the glass transition temperature(s) of the blends. In this paper we will summarize the many conclusions from our previous work in order to compare the results with the theoretical predictions of reference 28. We will show that all the effects observed can be explained on the basis of this theoretical approach.

EXPERIMENTAL

Materials

Three model systems have been investigated: poly(ethylene-*co*-vinyl acetate) (EVA)/solution chlorinated

* To whom correspondence should be addressed

Table 1 Characteristics of the polymers used[a]

Blend	Polymer	M_w (kg mol^{-1})	T_g (°C)	n	η^b (kPa s)
1	EVA	70	−25	1.42	16
	SCPE1	300	30	1.51	210
2	PBA	76	−40	1.465	0.01
	SCPE2	240	48	1.51	640
3	PS1	330	107	1.59	∝
	PVME	89	−30	1.466	0.18
4	PS2	65	100	1.59	∝
	PVME	89	−30	1.466	0.18

[a] M_w, weight-average molecular weight; n, index of refraction; η, viscosity
[b] Viscosities were measured at 95°C and $\dot{\gamma} \simeq 0.8\ s^{-1}$

polyethylene (SCPE1), poly(butyl acrylate) (PBA)/SCPE2 and polystyrene (PS)/poly(vinyl methyl ether) (PVME). The latter was also investigated as a function of the molecular weight of the PS (PS1 and PS2). The characteristics of each of the polymers are shown in *Table 1* where the four systems have been coded blend 1, blend 2, blend 3 and blend 4. Clear films of each blend were prepared by solvent casting and further details on the sample preparation procedure can be found elsewhere[23,25].

Apparatus

The details of the flow–light scattering apparatus have been described elsewhere[23]. The sample is located between two parallel glass plates, the bottom one fixed and the top one free to rotate with a speed controlled by the motor and gear mechanism. The cell can be heated at a constant heating rate or kept at a chosen fixed temperature. A hole through the metal allows a laser beam (He-Ne, $\lambda = 633$ nm) to impinge on the sample and the scattered radiation is then recorded by an array of photodiodes, whose signals, converted into digital values, are collected on a computer. The bottom section of the shear cell has an extended arm and is mounted on top of a freely rotating shaft. Measurements of torque are possible with the help of a displacement transducer attached to the extended arm and a calibrated leaf spring. Once a measurement is finished, the two glass plates can be released very rapidly to allow rapid quenching of the sample for further analysis.

For this parallel plate geometry, the shear rate depends on the radial distance as the top disc rotates at a constant angular speed Ω. The shear rate $\dot{\gamma}_r$ at a radius r is:

$$\dot{\gamma}_r = \Omega r/h \tag{4}$$

where h is the distance between the parallel plates. $\dot{\gamma}$ is zero at the centre ($r=0$) and a maximum at the outer edge of the plate. The values reported for the shear rate in the text correspond to those at a radial distance $r = 11$ mm which is the point at which the laser light was allowed to impinge on the sample.

RESULTS AND DISCUSSION

In our previous paper we investigated the effect of flow on the miscibility behaviour of the blends EVA/SCPE1, PBA/SCPE2, PS1/PVME and PS2/PVME. Detailed information on the results obtained can be found in reference 23 and here we will only outline the main conclusions of those measurements. In all three systems it was observed that the effect of flow was to induce phase separation at low shear rates (up to $\sim 5\ s^{-1}$) and then to enhance miscibility for higher shear rates. As an example, *Table 2* shows the effect of shear on shift in the cloud point temperatures, $\Delta T\ [\Delta T = T_c(\dot{\gamma}) - T_c(\dot{\gamma}=0)]$, for the blend EVA/SCPE1. A negative value of ΔT indicates that with shear, the phase boundary shifts towards lower temperatures which means that the immiscibility region becomes larger with shear. Correspondingly, a positive value of ΔT indicates shear-induced miscibility. It is clear from the table that for all compositions studied the effect of flow is to induce demixing at low shear rates and to induce mixing at higher shear rates and the same qualitative effects have been obtained for the two other blends.

From the results reported in reference 23 it also appeared that the bigger the mismatch in the viscosities of the two components of the blend, the larger the effect of shear on the miscibility behaviour of the system. For example, while the maximum drop in the cloud point temperature for the system EVA/SCPE1 in *Table 2* (which is the one for which the viscosities were more closely matched) was ~5°C, for the PS1/PVME (the largest mismatch in viscosities) the drop was almost 30°C. This effect has also been observed within the same blend but using different molecular weights and therefore different viscosities[25]. These results confirm Onuki's prediction about the effect of molecular weight on miscibility in which he proposed that the demixing effect would be larger the greater the difference in the molecular weights of the two polymers in the mixture[29]. The shear demixing effect was found to be composition dependent in the systems EVA/SCPE1 and PBA/SCPE2 (the system PS1/PVME was not studied as a function of blend composition). From the data it appeared that the larger the percentage of the higher viscosity component in the blend, the larger was the demixing effect.

Results obtained after the publication of reference 23 showed that if measurements were carried out up to higher temperatures than those in *Table 2*, further clearing and demixing of the samples occurred. These results were presented in a preliminary report[25], but for clarity we repeat them here in order to discuss carefully the theoretical interpretation. In all cases the samples were heated at 1°C min^{-1} under shear. It was found that if shear was applied from relatively low temperatures (~70°C) shear-induced demixing was observed as already reported. However if shear was

Table 2 Shift in the cloud point temperatures, ΔT, as a function of shear rate for the system EVA/SCPE1[19]

$\dot{\gamma}$ (s^{-1})	ΔT[a]			
	$\phi_{EVA}=0.4$	$\phi_{EVA}=0.5$	$\phi_{EVA}=0.6$	$\phi_{EVA}=0.7$
0	0	0	0	0
0.5	−2	−1.3	−0.9	−1.2
1.5	−4.5	−2.5	−0.9	−0.6
2.5	−1.3	−0.7	−0.4	0.1
3.5	–	1.9	0.3	0.5
4.0	–	3.2	0.6	0.8
7.0	–	–	3.2	1.8

[a] The values of ΔT were obtained by interpolation

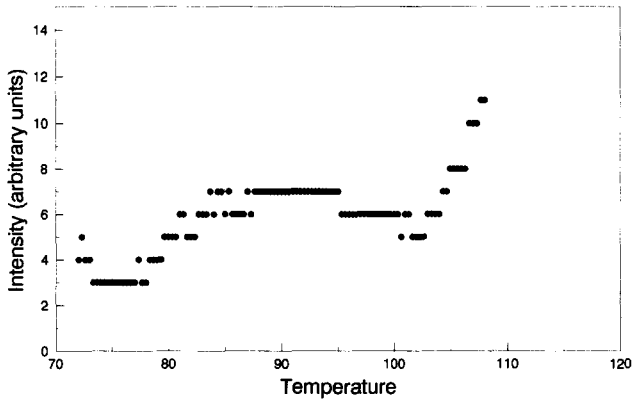

Figure 1 Plot of scattered intensity as a function of temperature for a PS1/PVME sample which is being sheared at 1°C min^{-1} and at a shear rate of 1.14 s^{-1}

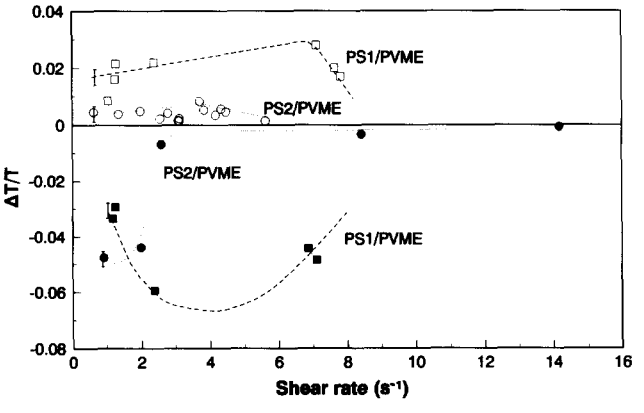

Figure 2 Normalized shift in the cloud point curve as a function of shear rate for the systems PS1/PVME (squares) and PS2/PVME (circles) in *Table 1*. The curves connecting the data points were chosen according to the qualitative theoretical dependencies shown in *Figure 4*. Representative error bars have been shown in each of the curves

started at higher temperatures (~90°C), shear-induced mixing was observed. In some cases, as the samples were heated under shear it was possible to observe, within the same experiment, shear-induced demixing followed by remixing and by shear-induced mixing as shown in *Figure 1*. *Figure 1* shows the scattered intensity from a PS1/PVME sample as a function of temperature as it was heated under shear at 1°C min^{-1} from 73°C at a shear rate equal to 1.14 s^{-1}. The quiescent cloud point temperature was 93.8°C but under shear the sample phase separated at ~79°C as reflected by the sharp increase in scattered intensity. The intensity increased with temperature up to 95°C and then decreased as the sample remixed. Finally, at 103°C the sample phase separated again. The sample therefore exhibited two cloud point temperatures, one at 79°C corresponding to shear-induced demixing and another at 103°C corresponding to shear-induced mixing.

As reported in reference 25, similar conclusions could be drawn from direct visual observation of quenched samples.

The data are summarized in *Figure 2*. Two different molecular weights of PS (PS1 and PS2) were used with the same sample of PVME. In each case two cloud points were observed. The solid symbols represent the cloud points observed at low temperatures and the open symbols those at high temperatures. In order to compare data for the different systems the shifts in the cloud point temperatures (ΔT) have been normalized by the cloud point temperatures themselves. The upper and lower cloud points were usually obtained in separate experiments on different samples of the same composition. For the lower cloud point the sample was preheated to ~70°C, the desired shear rate was applied and the sample then heated up to the cloud point. For the upper cloud point the sample was preheated to ~90–100°C, the desired shear rate was applied and the sample heated. In our previous discussion[23] we considered and discounted the possibility of explaining the results by experimental artifacts (such as viscous heating[30], deformation and break-up of droplets[31] or the migration of the lower molecular weight fractions to the regions of the sample where the stress is lower[23]). We consider the only explanation for the cloud point behaviour is an interaction between the rheology and the thermodynamic processes such that shear-induced mixing and/or demixing can occur in a single binary polymer blend depending on the temperature and shear rate used.

In the literature, the various authors have investigated the effect of flow on polymer miscibility by different techniques and the types of flow to which samples were subjected also vary from group to group. If we compare the results obtained by other authors[14,20,21] for the magnitude of the cloud point shift as a function of shear rate with our shear-induced mixing results (i.e. our second cloud point temperature), a reasonably good agreement is observed. Data for shear-induced demixing are much rarer, and we consider this is partly a consequence of the experimental procedures adopted by most other authors. In the literature it is common to first heat the sample and then apply shear, thus missing the lower cloud point completely.

The light scattering apparatus[23,25] was designed to allow fast release of samples at the end of an experiment so that they can be quenched and used for further study. In particular the samples were subjected to d.s.c. in order to observe the glass transition temperatures (T_gs). Typical results are shown in *Table 3* for a PS/PVME sample similar to blend 3, quenched from 80°C. By removing material from the sample disc at different radial distances from its centre, a whole range of shear rates can be obtained from one quenched sample. It is clear from *Table 3* that at this temperature, low shear rates (from near the centre of the disc) result in phase separation (two T_g values) while higher shear rates (outer edge of the disc) induce miscibility. The T_g results all confirm the light scattering data and are convincing evidence that the

Table 3 Glass transition temperatures[23] for a PS/PVME mixture similar but not identical to blend 3, quenched at 80°C from different radial positions (and therefore different shear rates) across the sample

$\dot{\gamma}$ (s^{-1})	No. of T_gs	T_{g1} (°C)	T_{g2} (°C)
0	1	−18.8	-
1.31	2	−21.4	−13
4.98	2	−24.9	−12
6.57	2	−21.4	−15.6
7.38	1	−19.3	-

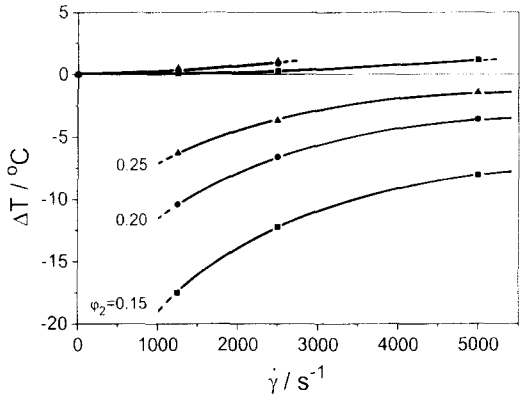

Figure 3 Shift of the cloud point temperature ΔT of a model solution of a polymer with 5000 segments and a *LCST*[28] as a function of the shear rate $\dot{\gamma}$ for the three compositions indicated by the volume fraction ϕ_2 of the polymer. The lower lines correspond to the lower temperature end of the island, and the upper lines to the main heterogeneous area

cloud point shifts reflect genuine thermodynamic mixing phenomena and not break up of domains until they are too small to scatter light. Similar results were obtained for the system EVA/SCPE1 where the sample morphology was tested by dynamic mechanical thermal analysis (d.m.t.a.). Specimens were tested in the tensile mode in the directions parallel and perpendicular to the shear flow. The results indicate that there is no significant orientation of the sample morphology due to the applied shear and this is to be expected given the low shear rates used here. Details of these measurements will be reported elsewhere[32].

In reference 28 we calculated phase diagrams for a polymer solution with a lower critical solution temperature (*LCST*). The model polymer contained 5000 segments. The calculated phase diagrams of the flowing polymer solution showed a peculiarity that has never been observed so far: closed miscibility gaps below the main heterogeneous area.

The theoretically calculated ΔT, the change of the cloud point temperature by the shear rate $\dot{\gamma}$ is plotted in *Figure 3*. The lower curves give the lower cloud point temperatures, they correspond to the low temperature side of the islands. The upper curves correspond to shear-induced mixing at the higher temperatures, these curves come to an end when the homogeneous area between the island and the original miscibility gap vanishes at a certain shear rate for a given composition. The line corresponding to the upper end of the islands is not shown.

The theoretical curves of *Figure 3* have to be compared with the experimental data of *Figure 2*. These two graphs look very similar: the original miscibility gap is lifted by the flow, i.e. shear-induced mixing occurs. This change of the cloud point temperature is given by the lines at $\Delta T > 0$. Simultaneously one observes a two-phase area in the homogeneous region of the phase diagram of the system at rest. The cloud points corresponding to this phenomenon are given by the lower lines in *Figures 2* and *3*.

There is however a difference between these two figures. The experimental curves of ΔT vs. $\dot{\gamma}$ for the blend (*Figure 2*) show a maximum in the upper curves and a minimum in the lower ones, while the curves obtained from the theoretical simulations (*Figure 3*) vary monotonically, i.e. they do not exhibit extrema. Very recent calculations[33] for a model polymer blend with a temperature dependent stored energy, which has been neglected in reference 27, yield a diagram that fits much better to the experimental curves of *Figure 2*.

Figure 4 gives a qualitative and schematic picture of the very complex shear influences on the phase separation behaviour of polymer blends, as determined from theoretical calculations. The projection of the heterogeneous areas (shaded) of the phase diagrams into the temperature–shear rate plane is plotted. In the unshaded area the blend is homogeneous in the whole composition range; in the shaded region it is demixed for some compositions. The demixing curve separating the areas of complete and incomplete miscibility breaks up into several parts because of the occurrence of the islands. In the presence of closed miscibility gaps (ranges of shear rates between the open and the solid squares in *Figure 4*) the system exhibits two cloud points. Starting from low temperatures the blend is homogeneous and becomes two-phase upon heating when the demixing curve is passed. This demixing upon heating is the same behaviour shown by the quiescent blend. Therefore all parts of the demixing curve where the system phase separates upon heating are called lines of normal demixing. Further raising of the temperature leads to a homogenization, the mixture leaves the area of the island and a part of the demixing curve is passed where the system mixes upon heating. The parts corresponding to this behaviour are called lines of contrary demixing, because here the blend demixes upon cooling. Finally the main heterogeneous region is reached and one observes a second cloud point when the demixing curve is crossed. When the island coalesces with the original miscibility gap (solid square in *Figure 4*) the line of contrary demixing has come to an end and the blend has only one cloud point.

The shear influences on the phase separation behaviour of polymer blends are now discussed starting from zero shear. First the miscibility gap shifts towards higher temperatures and one observes shear-induced mixing. At a certain $\dot{\gamma}$ an island shows up (open square) and coalesces with the main heterogeneous area at a higher $\dot{\gamma}$ (solid square). The line of contrary demixing crosses $\Delta T = 0$, i.e.

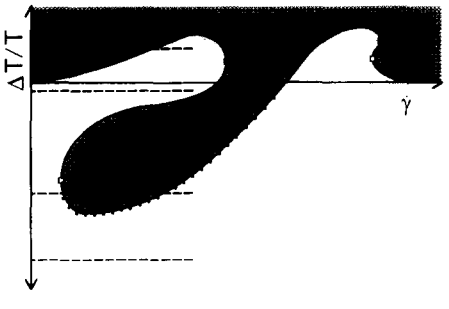

Figure 4 Schematic diagram showing the change of the phase separation behaviour of a polymer blend with the shear rate $\dot{\gamma}$: projection of the regions of possible phase separation (shaded area) into the $\Delta T/T$–$\dot{\gamma}$ plane. The open squares give the conditions at which the islands show up, and the solid squares where they coalesce with the main heterogeneous area. The broken lines indicate the values of temperature and shear rate at which the visual examinations of the samples were carried out, and the dotted parts of the demixing curve correspond to those shown in *Figure 2*

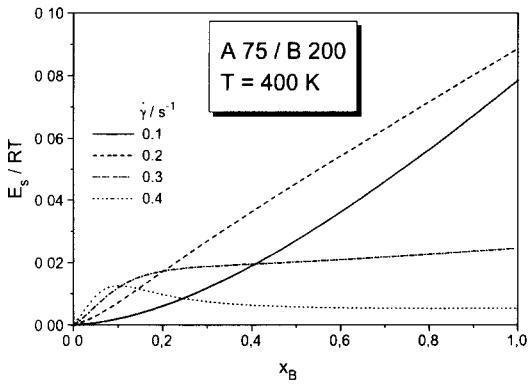

Figure 5 Reduced stored energy E_S/RT as a function of x_B, the mole fraction of component B, for the model system A75/B200 (the numbers give the molar masses of the components in kg mol^{-1}) from reference 27 (where all the equations and parameters can be found), at the indicated shear rates $\dot{\gamma}$

the shear effect changes its sign for the first time. At higher shear rates there is a region of plain shear-induced demixing which extends up to the second inversion of the effects, this time located on the line of normal demixing. Raising $\dot{\gamma}$ further one observes shear-induced mixing again, followed by a second regime (between the open and solid squares in *Figure 4*) where an island appears. After the coalescence of the two miscibility gaps, the shear influences fade away and the phase separation behaviour approaches that of the stagnant blend.

The shear effects on the phase separation behaviour can be understood knowing the shape of the stored energy as a function of the temperature and composition. As an example, E_S/RT is plotted as a function of x_B for one of the model systems of reference 27 (where all the equations and parameters can be found) in *Figure 5*. For low shear rates E_S grows monotonically with the content of the component B (higher molecular mass), i.e. the curvature is positive ($\partial^2 E_S/\partial x_B^2 > 0$) and shear-induced mixing is favoured. At a certain $\dot{\gamma}$ ($\sim 0.2\,s^{-1}$ for the presently discussed conditions) the disentanglement process starts in mixtures rich in B, where mixtures rich in A still show Newtonian behaviour. This leads to a peak in E_S, the curvature is negative ($\partial^2 E_S/\partial x_B^2 < 0$) over a great composition range and causes shear-induced demixing. The shear rate at which this process starts increases with temperature since the viscometric relaxation time decreases. With increasing $\dot{\gamma}$ the peak shifts to the low molecular mass side of the composition axis (the A75-rich side) and so the curvature of E_S at the concentrations where the solubility gap is located becomes positive again, i.e. shear-induced mixing takes place (in *Figure 5* for instance at $\dot{\gamma} = 0.4\,s^{-1}$).

A molecular explanation for this behaviour is provided by the entanglement concept. In stagnant mixtures the polymer chains are highly entangled, a temporary network exists, i.e. the liquid behaves like a rubber. The number of entanglements increases with the molar mass, and in mixtures it increases with the content of the high molar mass component (special influences of the chemical nature of the polymers are neglected). The ability of the blend to store energy is related to the number of entanglements. For low shear rates the number of entanglements is not influenced by flow. This leads to a monotonous growth of E_S with x_B. At the higher shear rates the number of entanglements decreases. The shear rate at which this process starts is the lower the larger x_B is. This leads to a new shape of E_S (x_B): for low x_B the behaviour does not change, E_S increases with x_B. At a certain composition the disentanglement process starts for the given shear rate and the increase of E_S is reduced; consequently the curvature becomes negative (the curve for $\dot{\gamma} = 0.2\,s^{-1}$ in *Figure 5*). For even higher shear rates E_S can pass a maximum since in the absence of entanglements no energy can be stored in the discussed entropic way (the curve for $\dot{\gamma} = 0.4\,s^{-1}$ in *Figure 5*).

In the following it will be briefly demonstrated how the dependence shown in *Figure 4* can be rationalized in terms of the generalized Gibbs energy [equation (1)]. As outlined above, one has to take the shape of E_S (x_B, T) at constant $\dot{\gamma}$ into consideration when discussing the changes of the phase diagram with $\dot{\gamma}$. Except for a certain temperature range, the stored energy acts towards the homogeneous state since the curvature of E_S (x_B) is positive. The limited temperature interval where the opposite is true shifts to higher temperatures with increasing $\dot{\gamma}$. This feature explains the occurrence of closed miscibility gaps within two ranges of shear in the following way.

The first islands ($\dot{\gamma}$ range between the left-hand pair of squares in *Figure 4*) show up at relatively low shear rates. They are induced at shear rates when the temperature range favouring shear-induced demixing is so near to the critical point that the influence of E_S can outweigh that of G_Z and phase separation is caused. The reason why the flowing system is homogeneous at somewhat higher temperatures, i.e. why an island shows up, is the fact that bogh G_Z and E_S act towards complete miscibility under these conditions. At higher shear rates this influence of shear-induced mixing shifts to temperatures so high that a demixing cannot be suppressed and the two heterogeneous domains coalesce. These islands are consequently created by E_S and seated below the equilibrium miscibility gap.

The second $\dot{\gamma}$ range (between the right-hand pair of squares in *Figure 4*) of islands lies in the region of the second shear-induced mixing. Here the temperature range where E_S acts towards shear-induced demixing is now located above T_c at a comparatively large distance from this value. At temperatures just below this range E_S favours shear-induced mixing very distinctly because of the large positive curvature of E_S. This influence can be so strong that the system becomes completely miscible. At lower temperatures, but still above T_c, the influence of E_S diminishes and that of G_Z becomes dominant, so that phase separation takes place. Again a closed miscibility gap is created; this time the island is entirely located above the critical temperature.

The scheme discussed above and shown in *Figure 4* can explain the experimental results given in *Figure 2* for the systems PS1/PVME and PS2/PVME. The curves of *Figure 2* correspond to the dotted parts of the demixing curve in *Figure 4*. The occurrence of shear-induced mixing and shear-induced demixing at the same shear rate can now be easily understood.

As mentioned earlier, samples in the light scattering apparatus can be released and quenched allowing further study. For each of these samples $\dot{\gamma}$ is zero at the centre and increases outwards. Thus a radius across the sample

corresponds to a horizontal line in *Figure 4*. A scheme of samples for a system similar to PS1/PVME, quenched from four temperatures is shown as Figure 4 in reference 25 and the temperature–shear rate areas corresponding to this experiment are indicated by dotted lines in *Figure 4* of the present paper. Visual observation of the quenched samples confirms the predictions of the phase diagram. At the lowest temperature, 51°C, the sample was clear. At the next temperature, 78°C, the sample was clear at the centre and at the outer edge and cloudy at the intermediate ranges. As seen in *Figure 4*, the sample cuts across the lower miscibility gap. The next sample was quenched from 82°C and was clear, while the final one, quenched from 100°C, was cloudy at the centre becoming progressively clearer towards the outer edge; both of these results are in agreement with *Figure 4*.

At the lowest temperature (lowest broken line in *Figure 4*, 51°C in the experiment of ref. 25) the system is homogeneous for all shear rates, the influence of G_Z is too strong, and the peak in E_S cannot affect phase separation. The measurement carried out at the second temperature (second broken line in *Figure 4*, 78°C in ref. 25) passes the island zone of shear-induced demixing at the intermediate shear rates. The third isotherm (third broken line in *Figure 4*, 82°C in ref. 25) lies completely in the homogeneous region, below the main heterogeneous area and above the islands. The fourth temperature (highest broken line in *Figure 4*, 100°C in ref. 25) is above the cloud point of the quiescent blend. Therefore the system is two-phase at zero shear and at low $\dot{\gamma}$ values, while for the higher shear rates one observes shear-induced mixing.

The second inversion in *Figure 4*, i.e. the point of intersection of the demixing curve and of the line given by $\Delta T=0$, where the effect of flow changes from shear-induced demixing to shear-induced mixing, is also found experimentally with the system EVA/SCPE1. The corresponding results are shown in *Table 2*. This blend shows shear-induced demixing for lower shear rates and shear-induced mixing (positive ΔT) for higher shear rates, which is the behaviour at the second inversion.

The comparison of the experimental and theoretical curves shows that the experimentally observed coincidence of shear-induced mixing and shear-induced demixing at one $\dot{\gamma}$ is simply explained by the theoretically predicted occurrence of closed miscibility gaps[30] below the main heterogeneous area in the phase diagrams of sheared polymer blends.

From the results presented here it is clear that the imposition of even very low shear rates has marked and complex effects on the miscibility of polymer blends. Further measurements will extend our studies over a range of blends with a view to classifying the most important parameters. At the same time we will extend our measurements to conditions nearer to those encountered in processing devices such as extruders and moulding machines, i.e. high shear rates and extensional flow.

ACKNOWLEDGEMENTS

The authors wish to thank Dr I. A. Hindawi for his light scattering measurements on the system EVA/SCPE1 and for the d.s.c. results, and the SERC and the Deutsche Forschungsgemeinschaft for financial support.

REFERENCES

1 Utracki, L. A. 'Polymer Alloys and Blends', Hanser, New York, 1989
2 Olabisi, O., Robeson, L. M. and Shaw, M. T. 'Polymer–Polymer Miscibility', Academic Press, London, 1978
3 Hashimoto, T., Kumaki, J. and Kawai, H. *Macromolecules* 1983, **16**, 641
4 Snyder, H. L., Meakin, P. and Reich, S. *Macromolecules* 1983, **16**, 757
5 Hill, R. G., Tomlins, P. E. and Higgins, J. S. *Macromolecules* 1985, **18**, 2555
6 Fruitwala, H., Higgins, J. S. and Tomlins, P. E. *Macromolecules* 1989, **22**, 3674
7 Fernandez, M. L., Higgins, J. S. and Tomlins, P. E. *Polymer* 1989, **30**, 3
8 Guo, W. and Higgins, J. S. *Polymer* 1991, **31**, 699
9 Rangel-Nafaile, C., Metzner, A. and Wissburn, K. *Macromolecules* 1984, **17**, 1187
10 Hindawi, I. A. *PhD Thesis*, Imperial College, 1991
11 Kramer-Lucas, H., Schenck, H. and Wolf, B. A. *Makromol. Chem.* 1988, **189**, 1613, 1627
12 Mazich, K. A. and Carr, S. H. *J. Appl. Phys.* 1983, **54**, 5511
13 Rector, L. P., Mazich, K. A. and Carr, S. H. *J. Macromol. Sci.-Phys. B* 1988, **27**, 421
14 Katsaros, J. D., Malone, M. F. and Winter, H. H. *Polym. Bull.* 1986, **16**, 83
15 Katsaros, J. D., Malone, M. F. and Winter, H. H. *Polym. Eng. Sci.* 1989, **29**, 1434
16 Lyngaae-Jorgensen, J. and Sondegaard, K. *Polym. Eng. Sci.* 1987, **27**, 344
17 Lyngaae-Jorgensen, J. and Sondegaard, K. *Polym. Eng. Sci.* 1987, **27**, 351
18 Cheikh Larbi, F. B., Malone, M. F., Winter, H. H., Halary, J. L., Leviet, M. H. and Monnerie, L. *Macromolecules* 1988, **21**, 3532
19 Hindawi, I., Higgins, J. S., Galambos, A. F. and Weiss, R. A. *Macromolecules* 1990, **23**, 670
20 Nakatani, A. I., Kim, H., Takahashi, Y., Matsushita, Y., Takano, A., Bauer, B. J. and Han, C. C. *J. Chem. Phys.* 1990, **93**, 795
21 Mani, S., Malone, M. F., Winter, H. H., Halary, J. L. and Monnerie, L. *Macromolecules* 1991, **24**, 5451
22 Mani, S., Malone, M. F. and Winter, H. *Macromolecules* 1992, **25**, 5671
23 Hindawi, I. A., Higgins, J. S. and Weiss, R. A. *Polymer* 1992, **33**, 2522
24 Larson, R. G. *Rheol. Acta* 1992, **31**, 497
25 Fernandez, M. L., Higgins, J. S. and Richardson, S. M. *Trans. IChemE* 1993, **71A**, 239
26 Wolf, B. A. *Macromolecules* 1984, **17**, 615
27 Horst, R. and Wolf, B. A. *Macromolecules* 1992, **25**, 5291
28 Horst, R. and Wolf, B. A. *Macromolecules* 1991, **24**, 2236
29 Onuki, A. *Phys. Rev. Lett.* 1989, **62**, 2472
30 Pearson, J. R. A. 'Mechanics of Polymer Processing', Elsevier Science, London, 1985, pp. 174–177
31 Han, C. D. 'Multiphase Flow in Polymer Processing', Academic Press, London, 1985, Ch 5
32 Fernandez, M. L., Higgins, J. S. and Richardson, S. M. 'Proceedings of the International Conference on Advances in Materials and Processing Technologies (AMTP '93)', Dublin City University, 24–27 August, 1993
33 Horst, R. and Wolf, B. A. *Macromolecules* 1993, **26**, 5676